

# Familial Alzheimer's disease in kindreds with missense mutations in a gene on chromosome 1 related to the Alzheimer's disease type 3 gene

E. I. Rogaev\*, R. Sherrington\*, E. A. Rogaeva\*, G. Levesque\*, M. Ikeda\*, Y. Llang\*, H. Chi\*, C. Lin\*, K. Holman\*, T. Tsuda\*, L. Mar†, S. Sorbi‡, B. Nacmias‡, S. Placentini‡, L. Amaducci‡, I. Chumakov§, D. Cohen§, L. Lannfelt||, P. E. Fraser\*, J. M. Rommens† & P. H. St George-Hyslop\*¶

\* Centre for Research into Neurodegenerative Diseases, Departments of Medicine (Neurology) and Medical Biophysics, University of Toronto, Toronto, and Division of Neurology, Department of Medicine, The Toronto Hospital, Toronto, Ontario M5S 1A8, Canada

† Research Institute, The Hospital for Sick Children, and Department of Molecular and Medical Genetics, University of Toronto, Toronto, Ontario M5S 1A8, Canada

‡ Department of Neurology and Psychiatry, University of Florence, viale Morgagni 85, Florence, Italy

§ Centre d'Etude Polymorphisme Humaine, 27 rue Juliette Dodu, 75010, Paris, France

|| Department of Clinical Neuroscience (Geriatric Medicine), Huddinge Hospital, Karolinska Institute, 14186 Huddinge, Sweden

¶ To whom correspondence should be addressed

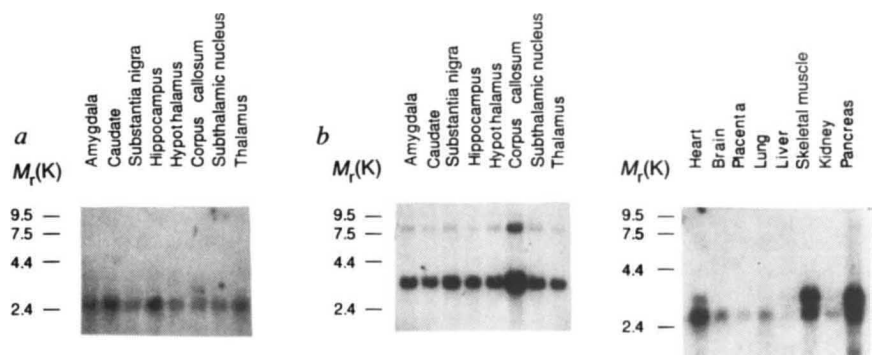
WE report the cloning of a novel gene (*E5-1*) encoded on chromosome 1 which has substantial nucleotide and amino-acid sequence similarity to the *S182* gene on chromosome 14q24.3. Mutations, including three new missense mutations in the *S182* gene, are associated with the *AD3* subtype of early-onset familial Alzheimer's disease (AD)<sup>1</sup>. Both the *E5-1* and the *S182* proteins are predicted to be integral membrane proteins with seven membrane-spanning domains, and a large exposed loop between the sixth and seventh transmembrane domains. Analysis of the nucleotide sequence of the open reading frame (ORF) of the *E5-1* gene led to the discovery of two missense substitutions at conserved amino-acid residues in affected members of pedigrees with a form of familial AD that has a later age of onset than the *AD3* subtype (50–70 years versus 30–60 years for *AD3*). These observations imply that the *E5-1* gene on chromosome 1 and the *S182* gene on chromosome 14q24.3 are members of a family of genes (*presenilins*) with related functions, and indicates that mutations in conserved residues of *E5-1* could also play a role in the genesis of AD. Our results also indicate that still other AD susceptibility genes exist.

Initial studies of the *S182* gene suggested the existence of other genes with similar sequences<sup>1</sup>. Searches of nucleotide sequence database by using the BLASTX alignment program uncovered three expressed sequence-tagged sequences (ESTs) (T03796, and subsequently R14600 and R05907) with substantial homology to two different segments within the *S182* ORF ( $P < 5.4 \times 10^{-11}$  identity >69% over at least 100 contiguous base pairs)<sup>2</sup>. Oligonucleotide primers were designed from these ESTs, and used to generate probes to screen complementary DNA libraries. Four cDNAs (*E5-1*, *G1-1*, *cc32* and *cc54*) were identified ranging in size from 1 to 2.3 kilobases (kb). The nucleotide sequence of these clones confirmed that all were derivatives of the same 2.3-kb transcript (designated *E5-1*). The gene encoding the *E5-1* transcript was mapped to human chromosome 1 by using hybrid mapping panels and the CEPH mega-YAC physical map (yeast artificial chromosome (YAC) clones 750g7, 921d12, 787g12) (results not shown).

The *E5-1* cDNA clones detected a low-intensity ~2.3-kb transcript on northern blots containing messenger RNA from several tissues, including most regions of the brain (Fig. 1). However, in skeletal muscle, cardiac muscle and pancreas, the *E5-1* gene is expressed at higher levels as two different transcripts of ~2.3 and ~2.6 kb (which we have not yet sequenced) (Fig. 1). Both of the *E5-1* transcripts have sizes clearly distinguishable from that of the 2.7-kb *S182* transcript, and did not cross-hybridize with *S182* probes at high stringency<sup>1</sup>.

The longest ORF within the *E5-1* cDNA consensus nucleotide sequence predicted a polypeptide containing 448 amino acids (Fig. 2). BLASTP alignment analyses detected significant homology with SPE-4 of *Caenorhabditis elegans* ( $P = 3.5 \times 10^{-26}$ ; identity = 20–63% over five domains of at least 22 residues), and weak homologies to several other transmembrane proteins similar to those previously reported for *S182* (ref. 1). However, the most striking alignment of *E5-1* was found with the amino-acid sequence predicted for the *S182* protein. These proteins share 63% overall amino-acid sequence identity, and several domains show almost complete identity (61–95% in the transmembrane domains) (Fig. 2). Furthermore, all of the residues mutated in *S182* in subjects with *AD3*, including three new mutations, are conserved in the putative *E5-1* protein (Fig. 2). As expected, hydrophobicity analyses indicate that both proteins could also share a similar structural organization, and are predicted to contain at least seven hydrophobic putative transmembrane domains, and large acidic hydrophilic domains at the amino terminus and between TM6 and TM7 (Fig. 3). An additional similarity between the *E5-1* and *S182* genes exists in the patterns of alternative splicing of the respective RNA transcripts. Analysis of cloned *E5-1* products of the polymerase chain reaction after reverse transcription (RT-PCR) isolated by using RNA from several tissues, including skeletal muscle and brain, revealed alternative splicing at nucleotides 1,153–1,250, which encode amino acids 263–296 in the TM6→TM7 loop of the *E5-1* protein (Figs 2 and 3). These residues share near-identity (31/33) with the alternatively spliced residues 257–290 in the TM6→TM7 loop of *S182* (which correspond to exon 9) (Figs

FIG. 1 Transcription of the *E5-1* homologue was investigated by hybridization of the *E5-1* cDNAs to northern blots of mRNA from human brain regions (a) and several peripheral tissues (c). The *E5-1* transcript is smaller and less abundant than the *S182* transcript, which is shown hybridized to the same blot using identical conditions (b)<sup>2</sup>.



2 and 3). In brain, the longer isoforms are the predominant transcripts for both *E5-1* and *S182*. However, whereas the shorter *E5-1* isoform can also be recovered from brain, the *S182* isoform lacking exon 9 is prominent only in leukocytes (manuscript in preparation).

The most noticeable differences between the two putative proteins occur in the central hydrophilic portion of the TM6→TM7 loop (residues 304–374 of *S182*; 310–355 of *E5-1*), and in the N terminus (Fig. 3). The TM6→TM7 loop domain is also less highly conserved between the murine and human *S182* genes (identity=47/60 residues), and shows no similarity to the equivalent region of *SPE4* (Fig. 3 in ref. 1).

The strong overall similarity between *S182* and the *E5-1* gene products suggested that the *E5-1* gene might be the site of disease-causing mutations in a subset of AD pedigrees where linkage has been excluded from chromosomes 14, 19 and 21 (refs 3, 4). To test this, cDNAs corresponding to the *E5-1* transcript were amplified from lymphoblasts, fibroblasts or post-mortem brain tissue of affected members of 23 pedigrees with early-onset familial AD in which mutations in the *βAPP* and *S182* genes has previously been excluded by direct-sequencing studies. Examination of these RT-PCR products detected a heterozygous A→G substitution at nucleotide 1,080, which would cause a 239 Met→Val mutation in all four affected members of an extended pedigree of Italian origin (FLO10) with early-onset, pathologically confirmed familial AD (onset at 50 years) (Figs 2 and 4). A second heterozygous substitution (A→T at nucleotide 787) causing a 141 Asn→Ile missense mutation was found in affected probands of three out of four pedigrees of Volga German ancestry (represented by cell lines AG09369, AG09907, AG09952 and AG09905; Coriell Institute, Camden, New Jersey). The appearance of the same mutation in affected mem-

bers of three different Volga German pedigrees probably reflects a founder effect (additional cell lines from these families are not publicly available to prove intra-family segregation). The absence of the 141 Asn→Ile mutation in the fourth Volga German pedigree (AG09952) could be explained in two ways. The first is that the 141 Asn→Ile mutation is a benign polymorphism enriched in descendants of the original Volga German founders. The evolutionary preservation of the 141 Asn residue in the *S182/E5-1* family and the noticeably non-conservative nature of the Asn→Ile mutation argue against this. The alternative explanation is that subject AG09952 (who is aged 77 years) possesses another type of AD. This interpretation is supported by the fact that late-onset AD may affect at least 5% of the population older than 70 years (reviewed in ref. 5), and by the fact that while the Volga German populations are probably drawn from a limited number of founders, they are unlikely to represent a pure population isolate, particularly after emigration to North America in the last century<sup>6,7</sup>. This subject is also homozygous for the 4 allele of apolipoprotein E. Nevertheless, neither of the *E5-1* gene mutations was found in 284 normal Caucasian controls (Fig. 4), nor was either mutation present in affected members of pedigrees with the *AD3* type of AD. Moreover, both mutations would be predicted to cause substitution of residues that are highly conserved within the presenilin gene family (Fig. 2).

The discovery of a gene whose putative product shares substantial amino-acid and structural similarities with the *S182* gene product suggests that these genes may be functionally related. Further, the high degree of sequence identity in the conserved domains, and the clustering of mutations within those domains, argue that these domains may be critical either to correct intracellular targeting or more probably to a common function. The

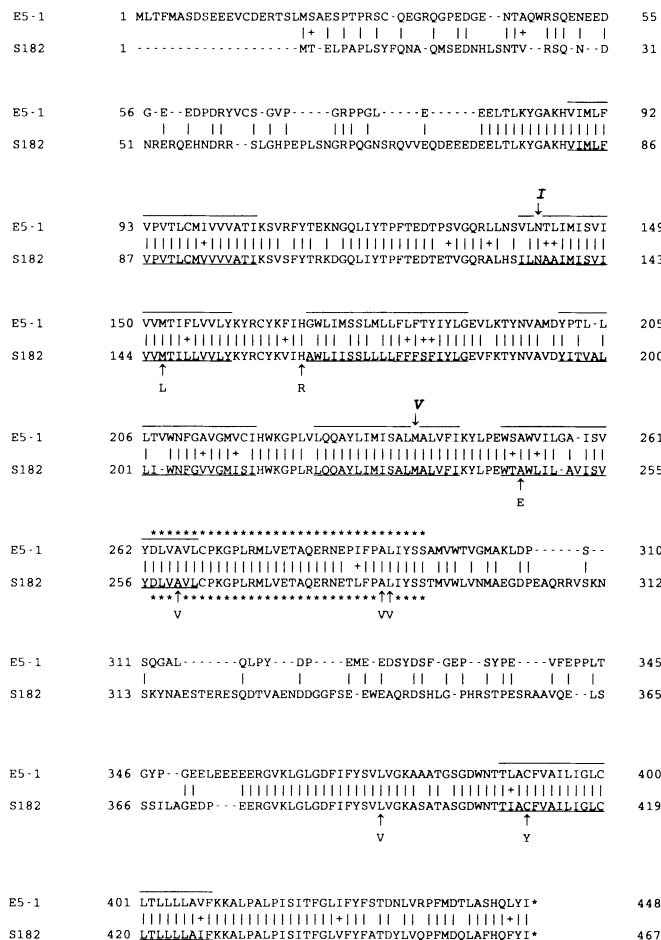
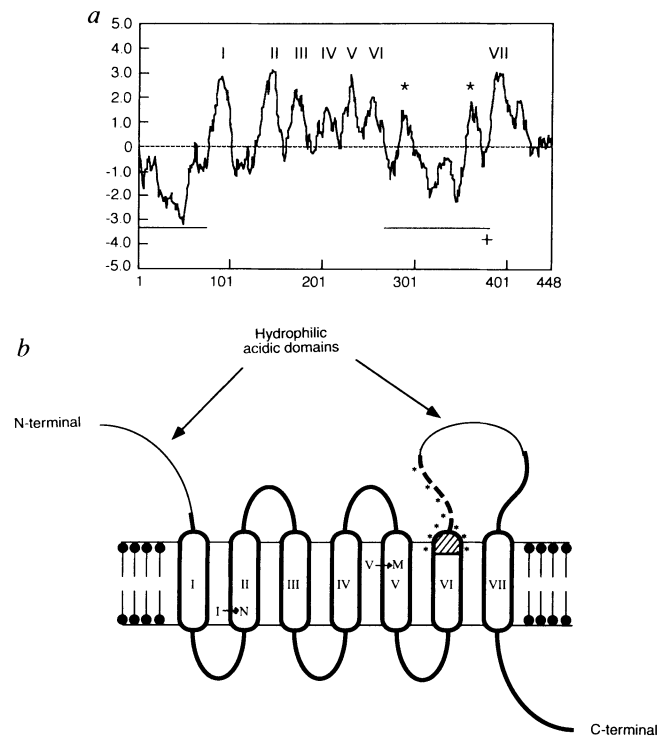
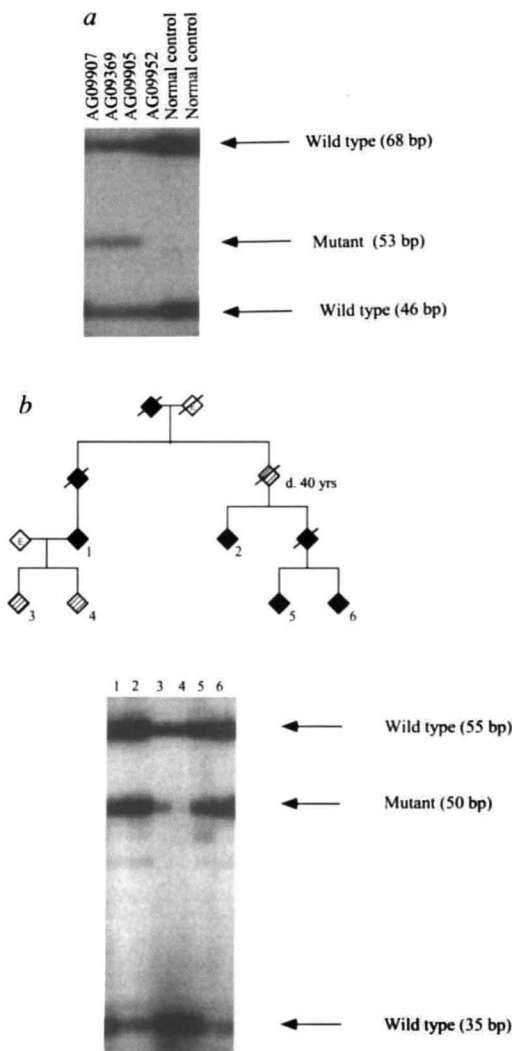


FIG. 2 Comparison of the predicted amino-acid sequence of the *E5-1* gene product (upper sequence) with that predicted for the *S182* gene product. Single-letter amino-acid codes are used, numbering from the first in-phase ATG codon which, for the *E5-1* gene, was surrounded by **GCC-agg-GCT-ATG**-c sequence which conformed to a translation start site. Identical residues are indicated by vertical lines, similar residues by +. The location of the putative mutations in the *E5-1* gene are indicated in bold type and by downward arrows above the *E5-1* sequence. The locations of the mutations in the *S182* gene are indicated by upward arrows below the *S182* sequence. Putative transmembrane (TM) domains are in open-ended boxes. The alternatively spliced exons are denoted by superscripted (*E5-1*) or subscripted (*S182*) asterisks. The nucleotide sequences have been deposited in the GSDB with accession numbers L42110 (*S182*) and L44557 (*E5-1*). The three new *S182* mutations were detected at 260 Ala→Val and 285 Ala→Val in two Japanese pedigrees, and at 392 Leu→Val in an Italian pedigree with early-onset familial AD (unpublished results). 260 Ala→Val and the 285 Ala→Val mutations: exon 9 was amplified from genomic DNA as previously described for the 286 Leu→Val mutation<sup>1</sup>. For the 260 Ala→Val mutation, end-labelled allele-specific oligonucleotides corresponding to the mutant sequence (994: 5'-GATTTAGTGGTTGTTTGTG) or the wild-type sequence (995: 5'-GATTAGTGGCTGTTTGTG) were hybridized at an annealing temperature of 48 °C, and washing was at 52 °C in 3 × SSC, 0.1% SDS<sup>1</sup>. For the 285 Ala→Val mutation, allele-specific oligonucleotides for the wild-type sequence (1,003: 5'-TTTTCCAGCTCTCATTTA) or the mutant primer (1,004: 5'-TTTTCCAGTTCTCATTTA) were hybridized at 48 °C and washed at 52 °C with 2 × SSC, 0.1% SDS. The Leu382Val mutation was scored by amplification of exon 13 from genomic DNA using oligonucleotides 996 (5'-AAACTTGGATTGGGAGAT) and 893 (5'-GTGTGGCCAGGGTAGAGAAGT) with PCR as described previously for the L286V mutation<sup>1</sup>. End-labelled wild-type oligonucleotide (999: 5'-TACAGTGTCTGGTTGGTA) or mutant oligonucleotide (1,000: 5'-TACAGTGTCTGGTTGGTA) were hybridized at 45 °C and then successively washed in 2 × SSC at 23 °C and then at 68 °C.



**FIG. 3** a, Hydrophobicity plot for the putative E5-1 polypeptide using the hydrophobicity indices of Kyte and Doolittle with a calculation window of 15 residues<sup>9</sup>. The seven putative TM domains are numbered I–VII (top). The two apolar domains within the TM6→TM7 loop, which could be either TM domains or membrane-associated structural components of the TM6→TM7 loop, are denoted by asterisks. Hydrophilic domains are underlined. A single putative *N*-linked glycosylation site is indicated by a cross at residue 405. The Thr 281 in S182 is changed to Pro 287 in E5-1 which obliterates the first putative glycosylation sequence observed in S182. Comparison with the same plot for the putative S182 protein shows virtual overlap if allowances are made for the differences in the sizes of the acidic hydrophilic domains at the N terminus and between TM6 and TM7 (ref. 1). b, Predicted structure of the E5-1 polypeptide. Sequences conserved between E5-1 and S182 are depicted by thick lines, divergent sequences by thin lines. The location of the alternatively spliced domain is depicted by a broken line with asterisks. In the sorter isoform, the hatched space within TM6 would be removed at residue Asp 263 and spliced to residue Ser 296, thereby reconstituting TM6. The approximate locations of the mutations are noted by single-letter amino acid codes, with the wild-type sequence on the right.

**FIG. 4** Missense mutation in the E5-1 open reading frame: a, 141 Asn→Ile; b, 239 Met→Val. RT-PCR products corresponding to the E5-1 ORF were generated from RNA of lymphoblasts or frozen post-mortem brain tissue by using oligonucleotide primer pairs 1,021: 5'-CAGAGGATGGAGAGAATAC and 1,018: 5'-GGTCCCCAAAAGTGCAT (product=888 bp); and 1,017: 5'-GCCCTAGTGTTTCATCAAGTA and 1,022: 5'-AAAGCGGGAGCCAAAGTC (product=826 bp) by PCR using 250  $\mu$ mol dNTPs, 2.5 mM MgCl<sub>2</sub>, 20 pmol oligonucleotides in 50  $\mu$ l, cycled for 40 cycles of 94 °C for 20 s, 58 °C for 20 s, 72 °C for 45 s. The PCR products were sequenced by automated cycle sequencing (ABI, Foster City, CA) and the fluorescent chromatograms were scanned for heterozygous nucleotide substitutions by direct inspection and by the Factura (version 1.2.0) and Sequence Navigator (version 1.0.1b15) software packages (results not shown). Missense mutations were confirmed and their absence in non-AD control subjects was ascertained in genomic DNA as follows. 141 Asn→Ile: the A→T substitution at nucleotide 787 creates a *Bcl*I restriction site. The exon bearing this mutation was amplified from 100 ng of genomic DNA using 10 pmol of oligonucleotides 1,041: 5'-CATTCACTGAGGACACACC (end-labelled) and 1,042: 5'-TGTAGAGCACCACCAAGA (unlabelled), with PCR reaction conditions similar to those described for 239 Met→Val. 2  $\mu$ l of the PCR product was restricted with *Bcl*I (NEBL, Beverly, MA) in 10  $\mu$ l reaction volume according to the manufacturer's protocol, and the products were resolved by non-denaturing PAGE (polyacrylamide gel electrophoresis). With wild-type sequences, the 114-bp PCR product is cleaved into 68-bp and 46-bp fragments, whereas mutant sequences yield three products of 53, 46 and 15 bp. Subjects AG09907, AG09369, AG09905 and AG09952 (lanes 1–4) are AD-affected subjects of Volga German ancestry (Coriell Institute, Camden, NJ); the remaining subjects are asymptomatic caucasian controls 239 Met→Val: the A→G substitution at nucleotide 1080 deletes a *Nla*III restriction site. Amplification of 100 ng of genomic DNA with 10 pmol oligonucleotides 1,034: 5'-GCATGGTGTGCATCCCACT, 1,035: 5'-GGACCACTCTGGGAGGTA: 0.5 U *Taq* polymerase, 250  $\mu$ M dNTPs, 1  $\mu$ Ci [ $\alpha$ -<sup>32</sup>P]dCTP, 1.5 mM MgCl<sub>2</sub>, 10  $\mu$ l volume; 30 cycles of 94 °C for 30 s, 58 °C for 20 s, 72 °C for 20 s, to generate a 110-bp product. 2  $\mu$ l of the PCR reaction were diluted to 10  $\mu$ l and restricted with 3 U of *Nla*III (NEBL) for 3 h. The restriction products were resolved by non-denaturing PAGE and visualized by autoradiography. Members of the FLO10 pedigree homozygous for wild-type sequences (products of 55, 35, 15 and 6 bp) or heterozygous for mutant sequences (products of 55, 50 and 6 bp) are shown.



nature of this function is unclear, but could reflect: (1) similar biochemical activities (perhaps with distinct substrate/ligand specificities); (2) different, perhaps consecutive, activities within the same biochemical pathway; or (3) subunits of a multimeric polypeptide like glutamate receptors<sup>8</sup>. The significant differences in the amino-acid sequences, and the occurrence of tissue-specific alternative splicing in the TM6→TM7 loop, suggest that this domain may be important, perhaps in determining gene-specific interactions.

A second conclusion derives from the observation of two different missense mutations in conserved domains of the E5-1 protein in subjects with a familial form of AD. The evidence associating mutations in *E5-1* to the cause of AD in some pedigrees is less rigorous than the link between similar mutations in *S182* and early-onset AD. Nevertheless, if these observations could be confirmed by the analysis of additional pedigrees, it would strengthen our hypothesis that the *S182* and *E5-1* gene products subserve the same biochemical pathway, and that perturbations in that pathway augment the risk for acquiring AD. Although the disease phenotypes in the pedigrees with *S182* mutations are generally similar to those with mutations in *E5-1*, there are subtle differences (*S182*, onset at age 30–50 years, duration 10 years; *E5-1*, onset at age 50–70 years; duration up to 20 years) (refs 6, 7 and S.S., unpublished results). These differences could be accounted for by the lower level of expres-

sion of the *E5-1* transcript in the central nervous system, by differences in tissue-specific alternative splicing of *E5-1*, or by a different specific activity of the *E5-1* gene product.

Finally, although our data indicate that still other AD-susceptibility genes exist, knowledge of the biochemical functions of both of these genes will probably be helpful in unravelling the processes that cause AD. □

Received 7 August; accepted 11 August 1995.

1. Sherrington, R. et al. *Nature* **375**, 754–760 (1995).
2. Altschul, S. F., Gish, W., Miller, W., Myers, E. W. & Lipman, D. J. *J. molec. Biol.* **215**, 403–410 (1990).
3. Schellenberg, G. D. et al. *Science* **258**, 668–670 (1992).
4. Lannfelt, L. et al. *Nature Genet.* **4**, 218–219 (1993).
5. Katzman, R. & Kawas, C. in *Alzheimer Disease* (eds Terry, R. D., Katzman, R. & Bick, K. L.) 105–122 (Raven, New York, 1994).
6. Cook, R. H. et al. *J. Neurology* **29**, 1402–1412 (1979).
7. Bird, T. D. et al. *Ann. Neurol.* **23**, 25–31 (1988).
8. Hollmann, N. & Heineman, S. A. *Rev. Neurosci.* **17**, 31–108 (1994).
9. Kyte, J. & Doolittle, R. F. *J. molec. Biol.* **157**, 105–132 (1982).

ACKNOWLEDGEMENTS. E.I.R., R.S. and E.A.R. contributed equally to this work. This work was supported by the Alzheimer Association of Ontario, Canadian Genetic Diseases Network, Medical Research Council of Canada, American Health Assistance Foundation, National Institute of Neurologic Disease and Stroke, the Scottish Rite Charitable Foundation, and the Eva Gordon Memorial Trust. P.StG.H. and J.M.R. are Scholars of the Medical Research Council of Canada. E.I.R. is on sabbatical leave from the Molecular Brain Genetics Laboratory, Research Centre of Mental Health, Moscow, Russia. Other support was obtained from, Consiglio Nazionale delle Ricerche (S.S., B.N., S.P. and L.A.), Glaxo Canada (R.S.), Tokai-Mitsui Research Foundation (T.T.), Helen B. Hunter Foundation (G.L. and H.C.). Cell lines used in this study were obtained from The Coreill Institute and The IADC National Cell Repository (no. P30 AG10133).

## Modulation of conscious experience by peripheral sensory stimuli

G. Bottini\*<sup>†‡</sup>, E. Paulesu\*<sup>§</sup>, R. Sterzi<sup>†</sup>,  
E. Warburton\*, R. J. S. Wise\*, G. Vallar<sup>||</sup>,  
R. S. J. Frackowiak\* & C. D. Frith\*<sup>¶</sup>

\* Wellcome Department of Cognitive Neurology, Institute of Neurology, and Medical Research Council Clinical Sciences Centre, Hammersmith Hospital, London, UK

† Divisione di Neurologia, Ospedale Niguarda Ca'Granda, 20138 Milano, Italy

§ INB CNR, Istituto Scientifico H San Raffaele, Università degli Studi, Milano, Italy

|| Dipartimento di Psicologia, Università la Sapienza, IRCCS, Clinica S. Lucia, Roma, Italy

¶ Psychology Department, University College London, London, UK

**LACK of awareness of touch associated with brain damage may transiently recover after stimulation of the vestibular system<sup>1,2</sup>. We used positron emission tomographic regional cerebral blood flow measurements to study the neurophysiological effect of vestibular stimulation on touch imperception in a subject with a right brain lesion. We tested the hypothesis that the vestibular system aids conscious tactile perception by introducing a bias in the neural system subserving body representation. We show that in normal subjects touch and vestibular signals share projections to the putamen, insula, somatosensory area II, premotor cortex and supra-marginal gyrus. In our patient a subset of these regions (right putamen and insula) was spared by the lesion and was maximally active when touch and vestibular stimulations were combined. These results support the suggestion that our phenomenological consciousness is associated with activation in circumscribed brain areas specific to the particular sensation of which we are aware.**

† To whom correspondence should be addressed at Divisione di Neurologia, Ospedale Niguarda Ca'Granda, 20138 Milano, Italy.

In this experiment we were interested in studying how perceptual awareness can be modulated by peripheral stimulation. Our model capitalizes on the observation that touch imperception caused by cerebral damage may transiently recover after appropriate caloric stimulation of the vestibular system<sup>1,2</sup>. The modulatory effect of caloric vestibular stimulation on touch imperception suggests that vestibular and touch projections may, to some extent, overlap in the brain. We have explored this hypothesis in four normal adult right-handed males who underwent 12 positron emission tomographic (PET) measurements of regional cerebral blood flow (rCBF), an index of synaptic activity<sup>3,4</sup>.

Two subjects received light, short tactile stimuli of the left hand during each of 6 of their 12 scans. Tactile stimulation was delivered by the examiner with the tip of the index finger every 2 s during PET scans. Subjects explicitly confirmed after each scan that they had consistently perceived the tactile stimuli. The area stimulated was the centre of the fourth metacarpal space of the left hand because this stimulus was previously used in an experiment showing transient remission of tactile imperception following cold vestibular stimulation (cold water was poured in the outer ear) in brain-damaged patients<sup>1</sup>. The other two subjects had left caloric vestibular stimulation before 6 of their 12 scans. Left vestibular stimulation with cold water was delivered for 30 s and stopped 10 s before the beginning of scanning, which coincided with arrival of radioactivity in the head. Therefore, tactile components of caloric stimulation did not contaminate the scan signal as the method is blind to brain activity occurring before the arrival of blood flow tracer in the brain<sup>4</sup>. The scans thus captured brain activity caused by vestibular symptoms only, which come on after a short delay from starting caloric stimulation and persist for a minute or so after it ceases<sup>5</sup>. After scan completion we confirmed that subjects showed the typical tonic deviation of gaze towards the side of cold stimulation and elicited explicit reports of transient dizziness and vertigo. rCBF was also measured six times during an eyes-closed resting state (baseline condition) in all four subjects. The order of the experimental and control scans was counterbalanced in both experiments to avoid habituation effects.

Anatomical overlap between touch and vestibular pathways